

Time-invariant entanglement and sudden death of non-locality

Bi-Heng Liu,^{1,2} Xiao-Min Hu,^{1,2} Jiang-Shan Chen,^{1,2} Chao Zhang,^{1,2} Yun-Feng Huang,^{1,2} Chuan-Feng Li,^{1,2,*} Guang-Can Guo,^{1,2} Göktuğ Karpat,^{3,4} Felipe F. Fanchini,⁴ Jyrki Piilo,³ and Sabrina Maniscalco^{3,†}

¹Key Laboratory of Quantum Information, University of Science and Technology of China, CAS, Hefei, 230026, People's Republic of China

²Synergetic Innovation Center of Quantum Information and Quantum Physics,

University of Science and Technology of China, Hefei, 230026, People's Republic of China

³Turku Center for Quantum Physics, Department of Physics and Astronomy, University of Turku, FIN-20014 Turku, Finland

⁴Faculdade de Ciências, UNESP - Universidade Estadual Paulista, Bauru, SP, 17033-360, Brazil

We investigate both theoretically and experimentally the dynamics of entanglement and non-locality for two qubits immersed in a global pure dephasing environment. We demonstrate the existence of a class of states for which entanglement is forever frozen during the dynamics, even if the state of the system does evolve. At the same time non-local correlations, quantified by the violation of the Clauser-Horne-Shimony-Holt (CHSH) inequality, either undergo sudden death or are trapped during the dynamics.

PACS numbers: 03.65.Yz, 03.65.Ta, 03.67.Mn

Introduction—Understanding correlations of genuine quantum nature is essential both for fundamentals of quantum theory and for applications of quantum information science. Recent studies have revealed that there exists numerous different types of purely non-classical correlations among the constituents of composite quantum systems, and they all prove to be relevant in the implementation of various tasks [1, 2]. Among them, entanglement can be argued to be the most fundamental. Apart from being a concept as old as quantum theory itself, entanglement is the main resource of quantum computation and quantum information processing [1]. Realistic quantum systems are, however, very sensitive to their surroundings [3] and, as a consequence, their characteristic quantum traits tend to rapidly disappear. In fact, under certain conditions, entanglement can be lost completely in a finite time rather than asymptotically, a phenomenon known as the sudden death of entanglement [4].

Given that a realistic quantum computing device has to be resilient against the destructive effects of the environment, strategies aimed at preserving entanglement as long as possible are of great practical importance. Motivated by this challenge, several methods have been proposed to protect the correlations in the system of interest from the undesirable noise. Examples are memory effects stemming from non-Markovian environments [5], dynamical decouplings techniques [6] and quantum Zeno effect [7]. In addition, it has been shown that certain quantum correlations, e.g. quantum discord, might forever freeze throughout the dynamics of the system under a suitable local noise setting, becoming time-invariant [8]. On the other hand, despite the fact that the phenomenon of time-invariant entanglement has been first noticed for a hybrid qubit-qutrit system in case of a simple global pure dephasing noise [9], a more complete characterization has been obtained only very recently under a rather general global dephasing scenario for a family of two qubit states having maximally mixed marginals, i.e., the Bell-diagonal states [10].

Another manifestation of non-classical correlations is related to the concept of quantum non-locality, stating that the predictions of quantum theory cannot be simulated by a lo-

cal hidden variable model. In the case of bipartite systems, non-local correlations can be identified through the violation of Bell inequalities [11]. It is well known that all pure entangled states of two qubits violate a Bell inequality [12] but this result no longer holds for mixed states [13]. In particular, even though entanglement is necessary for the existence of non-local correlations, there are entangled mixed bipartite states that do not violate Bell inequalities, i.e., whose correlations can be reproduced by a local hidden variable model. In order to investigate whether quantum correlations quantified by entanglement are classically reproducible or not, one can make use of a simple version of the Bell inequalities in the form of a Clauser-Horne-Shimony-Holt inequality [14]. The time evolution of CHSH violation in relation with the degree of entanglement in presence of decoherence has been studied both theoretically [15] and experimentally [16]. However, to the best of our knowledge, the sudden death of non-local correlations has not yet been experimentally verified.

In this work, we first theoretically study the time evolution of both entanglement and quantum non-locality, as quantified by concurrence and CHSH inequality violation, respectively, for Bell-diagonal states under a simple global pure dephasing model. We demonstrate that while the amount of entanglement remains time-invariant for a particular class of Bell-diagonal states, the degree of violation of quantum non-locality can suffer sudden death and thus disappear in a finite time interval. Then, we report on an experiment with photonic qubits demonstrating our theoretical results.

Theory— We consider two qubits globally interacting with classical stochastic dephasing noise along the z -direction. This noise can be thought as the representative of a class of interactions generating a pure dephasing process, with Hamiltonian $H(t) = -\frac{1}{2}n(t)(\sigma_z^A \otimes I^B + I^A \otimes \sigma_z^B)$, where σ_z is the usual Pauli spin operator in the z -direction, I is the identity operator, $n(t)$ is a stochastic noise field satisfying $\langle n(t) \rangle = 0$ and $\langle n(t)n(t') \rangle = \Gamma\delta(t-t')$, where $\langle \dots \rangle$ stands for ensemble average, and Γ is the damping rate associated with the stochastic field $n(t)$. The dynamics of the density matrix of the system is calculated as $\rho(t) = \langle U(t)\rho(0)U^\dagger(t) \rangle$, where

the ensemble averages is evaluated over the noise field, and the propagator is obtained as $U(t) = \exp[-i \int_0^t dt' H(t')]$. The resulting dynamics of the system can be expressed as [17]

$$\rho(t) = \begin{pmatrix} \rho_{11} & \rho_{12}\gamma & \rho_{13}\gamma & \rho_{14}\gamma^4 \\ \rho_{21}\gamma & \rho_{22} & \rho_{23} & \rho_{24}\gamma \\ \rho_{31}\gamma & \rho_{32} & \rho_{33} & \rho_{34}\gamma \\ \rho_{41}\gamma^4 & \rho_{42}\gamma & \rho_{43}\gamma & \rho_{44} \end{pmatrix}, \quad (1)$$

where ρ_{ij} denotes elements of the density matrix of the initial state and the decoherence factor reads $\gamma(t) = e^{-t\Gamma/2}$.

We now introduce the family of two qubits states that have maximally mixed reduced density matrices. Such states are known as Bell diagonal states and they are given as $\rho = (1/4)(I \otimes I + \sum_{j=1}^3 c_j \sigma_j \otimes \sigma_j)$, where σ_j are the Pauli operators, c_j are real numbers such that $0 \leq |c_j| \leq 1$, and the eigenvalues ($\lambda_k \geq 0$) of ρ are given by $\lambda_{1,2} = \frac{1}{4}(1 \mp c_1 \mp c_2 - c_3)$, $\lambda_{3,4} = \frac{1}{4}(1 \pm c_1 \mp c_2 + c_3)$. Bell diagonal states can be visualized as forming a tetrahedron with the four Bell states $|\phi^\pm\rangle = (|HH\rangle \pm |VV\rangle)/\sqrt{2}$ and $|\psi^\pm\rangle = (|HV\rangle \pm |VH\rangle)/\sqrt{2}$ sitting in the extreme points, as depicted in Fig. 1. If we consider the dynamics of the system, it is straightforward to observe that our global dephasing map preserves the form of the initial states and transforms their coefficients as follows:

$$\begin{aligned} c_1(t) &= \frac{1}{2}[c_1(1 + \gamma^4(t)) + c_2(1 - \gamma^4(t))], \\ c_2(t) &= \frac{1}{2}[c_1(1 - \gamma^4(t)) + c_2(1 + \gamma^4(t))], \\ c_3(t) &= c_3. \end{aligned} \quad (2)$$

As a consequence, $c_3(t)$ and also $[c_1(t) + c_2(t)]$ remain invariant throughout the dynamics, while both $c_1(t)$ and $c_2(t)$ asymptotically evolve to the same value, that is, $(c_1 + c_2)/2$.

Let us note that concurrence [18] of the family of Bell diagonal states can simply be expressed as

$$E(\rho) = 1/2 \max\{0, |c_1| + |c_2| + |c_3| - 1\}, \quad (3)$$

which implies that inside the tetrahedron in Fig. 1, there exists an octahedron representing the region of separable states defined by the condition $|c_1| + |c_2| + |c_3| \leq 1$. Therefore, the entangled Bell-diagonal states reside in the four remaining regions that are connected to each of the four Bell states at the edges. We also note that the surfaces of constant entanglement are given by the planes that are parallel to the faces of the octahedron containing the subset of separable states. The four regions of entanglement can be distinguished based on the sign of the three real coefficients defining the Bell diagonal states. Looking at Fig. 1, it is not difficult to see that in the red and orange entangled regions (which are connected to the Bell states $|\psi^+\rangle$ and $|\psi^-\rangle$ respectively at the extreme points), the coefficients c_1 and c_2 have the same sign. On the other hand, in the remaining two entangled regions, they have the opposite sign. Recalling that the considered global dephasing dynamics leaves $c_3(t)$ and $[c_1(t) + c_2(t)]$ unchanged in time and taking into account Eq. (3), we conclude that entanglement remains forever frozen throughout the time evolution

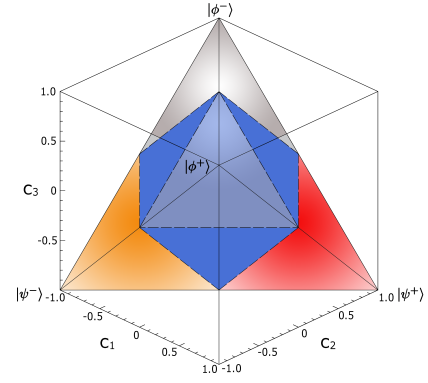


FIG. 1: Geometry of Bell-diagonal States. The blue octahedron in the middle, marked with dashed lines, represents the set of separable Bell-diagonal states. The states filling the red and orange regions, connected to the Bell states $|\psi^+\rangle$ and $|\psi^-\rangle$ respectively, give rise to time-invariant entanglement under global dephasing noise.

for the initial states residing in red and orange regions. To put it differently, whereas an initial state will have its c_3 constant, it will evolve towards $c_1 = c_2$ plane as t goes to infinity. Thus, the initial states from the red and orange regions will stay in the same region following a path towards the $c_1 = c_2$ plane on which entanglement is constant. Besides, the initial states from the other two regions will cross into the separable octahedron in finite time suffering sudden death of entanglement. The only exception to the sudden death of entanglement is the case $c_3 = 1$, where entanglement decays asymptotically to zero since these states will reach both the $c_1 = c_2$ plane and the region of separability simultaneously.

Motivated by the peculiar phenomenon of time-invariant entanglement, we will now investigate the violation of the CHSH inequality. After all, just as the presence of entanglement in the system, the violation of the CHSH inequality is also a manifestation of non-classicality. In order to study the non-local correlations, we first introduce the matrix $T = T_{ij} = \text{Tr}(\rho(\sigma_i \otimes \sigma_j))$ and the CHSH operator $B_{CHSH} = \vec{a} \cdot \vec{\sigma} \otimes (\vec{b} + \vec{b}') \cdot \vec{\sigma} + \vec{a}' \cdot \vec{\sigma} \otimes (\vec{b} - \vec{b}') \cdot \vec{\sigma}$, where \vec{a} , \vec{a}' and \vec{b} , \vec{b}' denote the unit vectors indicating the measurements on the first and the second qubits, respectively. The CHSH inequality is then given by $|\text{Tr}(\rho B_{CHSH})| \leq 2$. Optimizing over all measurements configurations, the maximum mean value of the CHSH operator for a given state ρ has been obtained as $\max |\text{Tr}(\rho B_{CHSH})| = 2\sqrt{M(\rho)}$ [19]. Here, $M(\rho) = \max_{i < j} \{u_i + u_j\} \leq 2$ with u_j being the three eigenvalues of the matrix $U = T^T T$, which is constructed from the correlation matrix T and its transposition T^T . There exists a choice of measurement setting violating the CHSH inequality if and only if $M(\rho) > 1$. For the Bell diagonal states, the maximum mean value of the CHSH operator reads

$$B(\rho) = 2\sqrt{\max\{c_1^2 + c_2^2, c_2^2 + c_3^2, c_1^2 + c_3^2\}}. \quad (4)$$

In Fig. 2, we display the outcomes of our analysis for entanglement and non-local correlations with the help of

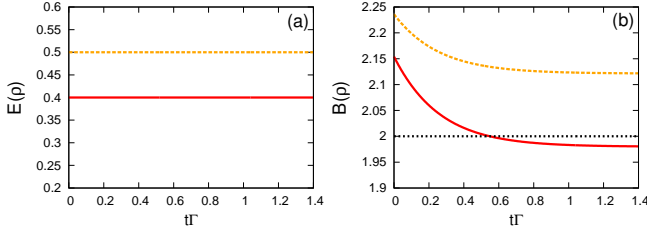


FIG. 2: (a) Entanglement quantified by concurrence $E(\rho)$ and (b) non-local correlations in terms of the maximum mean value of the CHSH operator $B(\rho)$ versus the dimensionless time $t\Gamma$. The initial Bell diagonal states are chosen as $c_1 = 1, c_2 = 0.4, c_3 = -0.4$ (red solid line) and $c_1 = c_3 = -0.5, c_2 = -1$ (orange dashed line). The black dotted line shows the non-locality threshold.

the CHSH inequality considering two different initial Bell-diagonal states under global dephasing noise. Whereas the red solid line corresponds to the initial state $c_1 = 1, c_2 = 0.4, c_3 = -0.4$, belonging to the red entangled region connected to the Bell state $|\psi^+\rangle$ as shown in Fig. 1, the orange dashed line stands for the initial state $c_1 = c_3 = -0.5, c_2 = -1$, which resides inside the orange entangled region connected to the Bell state $|\psi^-\rangle$. We see that the entanglement remains time-invariant for both initial states as expected. However, non-local correlations turn out to be susceptible to the harmful effects of the pure dephasing noise, unlike entanglement. In particular, for the former initial state, non-local correlations vanish in a finite time interval suffering sudden death. Hence, despite the invariance of entanglement in time, the system might even completely lose its non-classicality in terms of violation of the CHSH inequality.

Experiment— In our experimental scheme, the principal system of interest is represented by a pair of photons that are entangled in their polarization degrees of freedom. The polarization entangled photon pair is generated by a spontaneous parametric downconversion process. After a state preparation procedure, the photons are set to move along different arms and pass through quartz plates of adjustable thickness. As each of the photons passes through the quartz plate on its path, its polarization degrees of freedom locally couples to its frequency degrees of freedom, which acts as the local environment of the photon. Such an interaction induces a local unitary transformation, that is, $U_i(t_i)|\lambda\rangle \otimes |\omega_i\rangle = e^{in_\lambda\omega_i t_i}|\lambda\rangle \otimes |\omega_i\rangle$ where $|\lambda\rangle \otimes |\omega_i\rangle$ represents the state of the photon in arm i ($i = 1, 2$) with polarization $\lambda = H, V$ (horizontal or vertical) and frequency ω_i . Here, t_i is the time of interaction and n_λ is the refraction index of photons having polarization λ .

We suppose that the total state of the bipartite system and its environment can be initially written as a product state $|\Psi(0)\rangle = \rho(0) \otimes \int d\omega_1 d\omega_2 g(\omega_1, \omega_2)|\omega_1, \omega_2\rangle$, where $g(\omega_1, \omega_2)$ is the probability amplitude for the photon travelling along arm 1 to have frequency ω_1 and for the photon travelling along arm 2 to have frequency ω_2 . The corresponding joint probability distribution reads $P(\omega_1, \omega_2) = |g(\omega_1, \omega_2)|^2$. In this case, time evolution of the polarization state of the two

photons can be expressed as [20, 21]

$$\rho(t) = \begin{pmatrix} \rho_{11} & \rho_{12}\kappa_2 & \rho_{13}\kappa_1 & \rho_{14}\kappa_{12} \\ \rho_{21}\kappa_2^* & \rho_{22} & \rho_{23}\Lambda_{12} & \rho_{24}\kappa_1 \\ \rho_{31}\kappa_1^* & \rho_{32}\Lambda_{12}^* & \rho_{33} & \rho_{34}\kappa_2 \\ \rho_{41}\kappa_{12}^* & \rho_{42}\kappa_1^* & \rho_{43}\kappa_2^* & \rho_{44} \end{pmatrix}, \quad (5)$$

which represents a pure dephasing dynamics. The decoherence factors are given by $\kappa_1(t) = G(t_1, 0)$, $\kappa_2(t) = G(0, t_2)$, $\kappa_{12}(t) = G(t_1, t_2)$ and $\Lambda_{12}(t) = G(t_1, -t_2)$ with $G(t_1, t_2) = \int d\omega_1 d\omega_2 P(\omega_1, \omega_2) e^{-i\Delta n(\omega_1 t_1 + \omega_2 t_2)}$, being the Fourier transform of the joint probability distribution and $\Delta n = n_V - n_H$ denotes the birefringence.

Assuming that the joint probability distribution of the considered two photons is in a Gaussian form, i.e., $P(\omega_1, \omega_2) = (1/2\pi\sqrt{\det C}) e^{-\frac{1}{2}(\vec{\omega} - \langle\vec{\omega}\rangle)^T C^{-1}(\vec{\omega} - \langle\vec{\omega}\rangle)}$, where $\vec{\omega} = (\omega_1, \omega_2)^T$, $\langle\vec{\omega}\rangle = (\langle\omega_1\rangle, \langle\omega_2\rangle)^T$, and $C = C_{ij} = \langle\omega_i\omega_j\rangle - \langle\omega_i\rangle\langle\omega_j\rangle$ with $\langle\omega_1\rangle = \langle\omega_2\rangle = \omega_0/2$ and $C_{11} = C_{22} = \langle\omega_i^2\rangle - \langle\omega_i\rangle^2$, the decoherence function reads

$$G(t_1, t_2) = e^{\frac{i\omega_0}{2}\Delta n(t_1+t_2) - \frac{C_{11}}{2}\Delta n^2(t_1^2+t_2^2+2Kt_1t_2)}, \quad (6)$$

with $K = C_{12}/C_{11}$ being the correlation coefficient between the two frequencies. Note that, even though the interactions of the photons with their individual environments are local in this setting, the resulting dynamics can be non-local due to the strong initial correlations between the environmental degrees of freedom. Let us now set the interactions times to be identical, that is $t_1 = t_2 = t$, and consider the case of full anticorrelations between the frequencies, corresponding to $K = -1$. It is rather straightforward to observe in this case that $\Lambda_{12}(t) = e^{-2C_{11}\Delta n^2 t^2}$ and $\kappa_{12}(t) = e^{i\omega_0\Delta n t}$, and thus $|\kappa_{12}(t)| = |\kappa_{12}^*(t)| = 1$ at all times throughout the dynamics, which in turn effectively simulates a global pure dephasing dynamics creating a decoherence free subspace.

In Fig. 3, we describe our experimental setup. ES is a standard two photon entanglement source that generates the state $|\phi^+\rangle = (|HH\rangle + |VV\rangle)/\sqrt{2}$. After the creation of the polarization entangled photon pair, each photon is separated by a special designed tunable beam splitter (TBS) as shown in the dashed inset and travels along 5 m single mode fiber (L) or

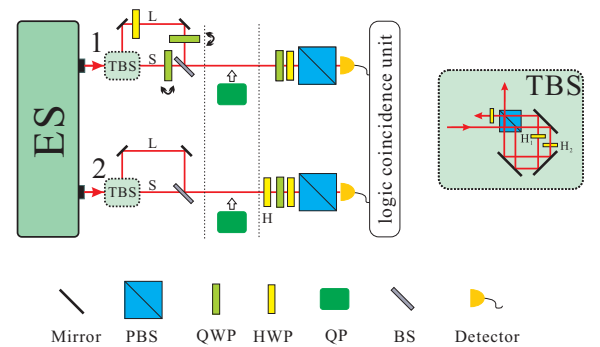


FIG. 3: Our experimental setup. PBS - polarizing beam splitter, QWP - quarter wave plate, HWP - half wave plate, QP - quartz plate, TBS - tunable beam splitter and ES - entangled photon source.

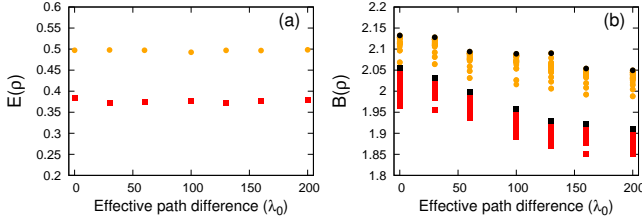


FIG. 4: (a) Entanglement and (b) CHSH inequality violation versus effective path difference. The experimentally prepared initial Bell diagonal states are $c_1 = 1, c_2 = 0.4, c_3 = -0.4$ (red squares) and $c_1 = c_3 = -0.5, c_2 = -1$ (orange circles). In (b), we show the violation of the CHSH inequality for many different measurement settings. The optimal violation is given by the highest points in the y-axis for each state, which are marked with black data points.

1 m single mode fiber (S) and then combined together at another beam splitter (BS). (The inset TBS contains a polarizing beam splitter (PBS) and three half wave plates (HWPs). The transmission reflection ratio is well adjusted by the two HWPs and the relative amplitude of L arm and S arm are well set.) The L part of the photon in arm 1 passes through a half wave plate set at 45° so that the two photons can be prepared in the Bell diagonal states $\alpha|\phi^\pm\rangle\langle\phi^\pm| + (1 - \alpha)|\psi^\pm\rangle\langle\psi^\pm|$. Here, the phase 0 or π can be set by tuning the quarter wave plate in arms L and S. In the next stage, each of the photons passes through quartz plates in different arms, and then the photon in arm 2 is rotated by another half wave plate H set at 45° , causing the dynamics to resemble the one described in Eq. (1), by transforming $|\phi^\pm\rangle$ and $|\psi^\pm\rangle$ into each other. Explicitly, after relabelling the elements of the initial state, the dynamics reads

$$\rho(t) = \begin{pmatrix} \rho_{11} & \rho_{12}\kappa_2^* & \rho_{13}\kappa_1 & \rho_{14}\Lambda_{12} \\ \rho_{21}\kappa_2 & \rho_{22} & \rho_{23}\kappa_{12} & \rho_{24}\kappa_1 \\ \rho_{31}\kappa_1^* & \rho_{32}\kappa_{12}^* & \rho_{33} & \rho_{34}\kappa_2^* \\ \rho_{41}\Lambda_{12}^* & \rho_{42}\kappa_1^* & \rho_{43}\kappa_2 & \rho_{44} \end{pmatrix}. \quad (7)$$

Finally, the resulting two photon state is analysed by the quantum state tomography or CHSH measurements.

In the experiment we use a CW laser (Toptica, wavelength is 404 nm and power is about 100 mW) to pump two type-I cut 0.3 mm thick BBO to prepare the maximally entangled states. The initial coincidence is about 6000/s and the final coincidence is about 350/s due to the fiber coupling loss and the efficiency of BS. The integration time is 150 s and the total coincidence is about 50000, which gives an error (here we only calculate the photon number statistic error) about 0.006 and 0.008 for concurrence and CHSH violation, respectively, for the Bell diagonal state with $c_1 = 1, c_2 = 0.4, c_3 = -0.4$. On the other hand, the integration time is 300 s and the total coincidence is about 100000, giving an error about 0.004 and 0.006 for concurrence and CHSH inequality, respectively, for the Bell diagonal state having $c_1 = c_3 = -0.5, c_2 = -1$.

Fig. 4 shows the outcomes of our experimental investigation for the experimentally prepared initial Bell diagonal states. More specifically, we display the behaviour of entanglement in (a) for the states having $c_1 = 1, c_2 = 0.4, c_3 =$

-0.4 and $c_1 = c_3 = -0.5, c_2 = -1$ with red squares and orange circles respectively, while (b) presents the results of the CHSH inequality violation for the same pair of states. Indeed, as we show the results for the degree of the CHSH inequality violation for many different measurement configurations in (b), the optimal violation is given by the highest point in the y-axis for each value of the effective path difference. By looking at Figs. 2 and 4, we observe that theoretical and experimental results are in good agreement with each other. The comparison between experimental data and theoretical predictions shows a less accurate match for the Bell inequality violation than for the entanglement dynamics. We believe that the reason lies in the fact that the CHSH violation with very sensitive correlation measurements is more vulnerable to experimental inaccuracies than quantification of entanglement with state tomography measurements. The experimental data do show, however, conclusive evidence of the fact that, under global dephasing noise, entanglement becomes forever frozen while non-local correlations can suffer sudden death and disappear in a finite time interval.

We lastly elaborate on how we experimentally test the violation of the Bell inequalities. We first reconstruct the density matrix using the standard techniques of two-qubit state tomography. Then, we numerically maximize the degree of violation of the CHSH inequality. Next, we fix all the wave plate angles (which correspond to different measurement bases) at the optimal values and individually change them one by one to check for the maximal experimental violation of the CHSH inequality. We repeat the same procedure for all the other states at each value of the effective path difference. In other words, at each time point, we search, within a certain angle interval, for the optimal experimental angles showing maximum violation of the CHSH inequality, in order to compensate for the uncertainties that might occur in the tomography process. As an example, we show the results of our analysis for the Bell diagonal state with the coefficients $c_1 = 1, c_2 = 0.4, c_3 = -0.4$ in Fig. 5. Note that in this case the optimal violation is indeed given by the angles obtained from the numerical optimization.

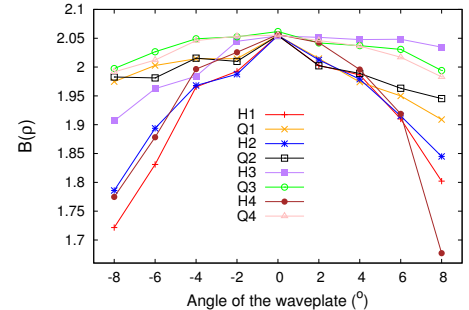


FIG. 5: Degree of CHSH inequality violation for different measurement configurations around the numerically calculated optimal angles for the Bell diagonal state with $c_1 = 1, c_2 = 0.4, c_3 = -0.4$. While H1 (H2, H3, H4) form the half wave plate of basis \vec{a} (\vec{a}' , \vec{b} , \vec{b}'), Q1 (Q2, Q3, Q4) form the quarter wave plate of basis \vec{a} (\vec{a}' , \vec{b} , \vec{b}').

Conclusion— In summary, we have presented a detailed examination of the dynamics of both entanglement and non-local correlations, quantified via concurrence and CHSH inequality violation respectively, under global pure dephasing noise for the set of Bell diagonal states. Our results demonstrate that, remarkably, while entanglement can become time-invariant throughout the time evolution for a certain subset of Bell diagonal states, non-local correlations in these states might vanish in a finite time suffering sudden death. Non-local correlations do not seem, according to our investigation, to display a time-invariant behaviour. However, they can reach a non-zero stationary value larger than two which will be maintained during the dynamics, as shown in Figs. 4 (b) and 2 (b). The existence of time-invariant entanglement and non-locality trapping may pave the way to new strategies, based on reservoir engineering techniques, aimed at exploiting rather than fighting decoherence.

This work was supported by the National Natural Science Foundation of China (Nos. 61327901, 11374288, 11474268, 61225025, 11274289, 11325419), the Strategic Priority Research Program (B) of the Chinese Academy of Sciences (Grant No. XDB01030300), the Fundamental Research Funds for the Central Universities, China (Grant Nos. WK2470000018 and WK2470000022), the National Youth Top Talent Support Program of National High-level Personnel of Special Support Program (No. BB2470000005). GK is supported by the São Paulo Research Foundation (FAPESP) under the grant numbers 2012/18558-5 and 2014/20941-7, and FFF under the grant number 2015/05581-7. FFF is also supported by the National Counsel of Technological and Scientific Development (CNPq) under the grant number 474592/2013-8 and by the National Institute for Science and Technology of Quantum Information (INCT-IQ) under the process number 2008/57856-6. CFL, JP and SM acknowledge financial support by the EU Collaborative project QuProCS (Grant Agreement 641277). JP and SM also acknowledge fi-

nancial support from the Magnus Ehrnrooth Foundation.

* Electronic address: cfl@ustc.edu.cn

† Electronic address: smanis@utu.fi

- [1] R. Horodecki, P. Horodecki, M. Horodecki, and K. Horodecki, *Rev. Mod. Phys.* **81**, 865 (2009).
- [2] K. Modi, A. Brodutch, H. Cable, T. Paterek, and V. Vedral, *Rev. Mod. Phys.* **84**, 1655 (2012).
- [3] H. -P. Breuer and F. Petruccione, *The Theory of Open Quantum Systems* (Oxford University Press, Oxford, 2007).
- [4] T. Yu, J.H. Eberly, *Phys. Rev. Lett.* **93**, 140404 (2004).
- [5] B. Bellomo, R. Lo Franco, and G. Compagno, *Phys. Rev. Lett.* **99**, 160502 (2007).
- [6] L. Viola and S. Lloyd, *Phys. Rev. A* **58**, 2733 (1998); L. Viola, E. Knill, and S. Lloyd, *Phys. Rev. Lett.* **82**, 2417 (1999).
- [7] S. Maniscalco, F. Francica, R. L. Zaffino, N. Lo Gullo, and F. Plastina, *Phys. Rev. Lett.* **100**, 090503 (2008).
- [8] P. Haikka, T. H. Johnson, and S. Maniscalco, *Phys. Rev. A* **87**, 010103(R) (2013).
- [9] G. Karpat and Z. Gedik, *Phys. Lett. A* **375**, 4166 (2011).
- [10] E. G. Carnio, A. Buchleitner, and M. Gessner, *Phys. Rev. Lett.* **115**, 010404 (2015).
- [11] J. S. Bell, *Physics* **1**, 195 (1964).
- [12] N. Gisin, *Phys. Lett. A* **154**, 201 (1991).
- [13] R. F. Werner, *Phys. Rev. A* **40**, 4277 (1989).
- [14] J. F. Clauser, M. A. Horne, A. Shimony, and R. A. Holt, *Phys. Rev. Lett.* **23**, 880 (1969).
- [15] L. Mazzola, B. Bellomo, R. Lo Franco, and G. Compagno, *Phys. Rev. A* **81**, 052116 (2010).
- [16] J.-S. Xu *et al.*, *Phys. Rev. Lett.* **104**, 100502 (2010).
- [17] T. Yu, J.H. Eberly, *Phys. Rev. B* **68**, 165322 (2003).
- [18] W. K. Wootters, *Phys. Rev. Lett.* **80**, 2245 (1998).
- [19] M. Horodecki, P. Horodecki, and R. Horodecki, *Phys. Lett. A* **200**, 340 (1995).
- [20] E.-M. Laine *et al.* *Phys. Rev. Lett.* **108**, 210402 (2012), Erratum: *ibid.* **111**, 229901 (2013).
- [21] B.-H. Liu *et al.*, *Sci. Rep.* **3**, 1781 (2013).